

**Certified Reduced Basis Methods for
Parametrized Parabolic
Partial Differential Equations with
Non–Affine Source Terms**

**Dirk Klindworth^a, Martin A. Grepl^{b,*}, and
Georg Vossen^a**

Bericht Nr. 324

April 2011

Key words: Reduced basis methods, parabolic PDEs,
non–affine parameter dependence, a *posteriori*
error estimation, empirical interpolation method,
welding process.

AMS subject classifications: 35K15, 35Q80, 65M15

**Institut für Geometrie und Praktische Mathematik
RWTH Aachen**

Templergraben 55, D–52056 Aachen (Germany)

^a RWTH Aachen University, Nonlinear Dynamics of Laser Processing, Steinbachstraße 15, 52074 Aachen, Germany.

^b RWTH Aachen University, Numerical Mathematics, Templergraben 55, 52056 Aachen, Germany.

* Corresponding author. Tel.: +49 241 8096470, Fax: +49 241 80696470
Email address: grepl@igpm.rwth-aachen.de (Martin A. Grepl)

Preprint submitted to Comput. Methods Appl. Mech. Engrg.

Certified Reduced Basis Methods for Parametrized Parabolic Partial Differential Equations with Non-Affine Source Terms

Dirk Klindworth^a, Martin A. Grepl^{b,*}, Georg Vossen^a

^a*RWTH Aachen University, Nonlinear Dynamics of Laser Processing, Steinbachstraße 15, 52074 Aachen, Germany*

^b*RWTH Aachen University, Numerical Mathematics, Templergraben 55, 52056 Aachen, Germany*

Abstract

We present rigorous *a posteriori* output error bounds for reduced basis approximations of parametrized parabolic partial differential equations with non-affine source terms. The method employs the empirical interpolation method in order to construct affine coefficient-function approximations of the non-affine parametrized functions. Our *a posteriori* error bounds take both error contributions explicitly into account — the error introduced by the reduced basis approximation *and* the error induced by the coefficient function interpolation. To this end, we employ recently developed rigorous error bounds for the empirical interpolation method and develop error estimation and adjoint procedures to provide rigorous bounds for the error in specific outputs of interest. We present an efficient offline-online computational procedure for the calculation of the reduced basis approximation and associated error bound. The method is thus ideally suited for many-query or real-time contexts. As a specific motivational example we consider a welding process. Our numerical results show that we obtain efficient and reliable mathematical models which may be gainfully employed in manufacturing and product development.

Keywords:

reduced basis methods, parabolic PDEs, non-affine parameter dependence, *a posteriori* error estimation, empirical interpolation method, welding process

1. Introduction

The role of numerical simulation in engineering and science has become increasingly important. System or component behavior is often modeled using a set of partial differential equations and

*Corresponding author. Tel.: +49 241 8096470, Fax: +49 241 80696470

Email address: grepl@igpm.rwth-aachen.de (Martin A. Grepl)

associated boundary and initial conditions, the analytical solution to which is generally unavailable. In practice, a discretization procedure such as the finite element method (FEM) is used.

However, as the physical problems become more complex and the mathematical models more involved, current computational methods prove increasingly inadequate, especially in contexts requiring numerous solutions of parametrized partial differential equations for many different values of the parameter. For example, the design, optimization, control, and characterization of engineering components or systems often require repeated, reliable, and real-time prediction of performance metrics, or outputs, s^e , such as heat fluxes or flow rates¹. These outputs are typically functionals of field variables, y^e , — such as temperatures or velocities — associated with a parametrized partial differential equation; the parameters, or inputs, μ , serve to identify a particular configuration of the component — such as boundary conditions, material properties, and geometry. The relevant system behavior is thus described by an implicit input-output relationship, $s^e(\mu)$, evaluation of which demands solution of the underlying partial differential equation (PDE). Even for modest-complexity models, the computational cost to solve these problems using classical discretization procedures is prohibitive.

More specifically, the motivation of this work is to develop an efficient mathematical model for the heat flow in a welding process [1, 2, 3, 4, 5]. An accurate knowledge of the temperature distribution within the workpiece is crucial in determining the quality of the weld: two such quality measures are the weld pool depth — indicating the strength of the joint — and the shape distortion of the workpiece.

A complete model of the welding process which couples and accounts for all of the physical processes involved does not yet exist. In actual practice, the heat flux input is therefore modeled as a parametrized volume heat source [6, 2, 7]. The temperature distribution, $y^e(x, t; \mu)$, within the workpiece is governed by the unsteady convection-diffusion equation

$$\frac{\partial}{\partial t} y^e(x, t; \mu) + \mathbf{v} \cdot \nabla y^e(x, t; \mu) - \kappa \nabla^2 y^e(x, t; \mu) = q(\mathbf{x}; \mu) u(t), \quad \mathbf{x} \in \Omega, t \in I, \quad (1)$$

with initial condition (say) $y^e(x, t = 0; \mu) = 0$. Here, $\Omega \subset \mathbb{R}^3$ is the spatial domain, a point in which shall be denoted by $x = (x_1, x_2, x_3)$, the time interval of interest is $I =]0, t_f]$ with final time

¹Here, superscript “e” shall refer to “exact.” We shall later introduce a “truth approximation” which will bear no superscript.

$t_f > 0$, v is the velocity, κ the thermal diffusivity, and $u(t)$ the source strength. In this paper, we consider the so called *hemispherical volume heat source* given by

$$q(x; \mu) := e^{-x_1^2/\sigma_1^2} e^{-x_2^2/\sigma_2^2} e^{-x_3^2/\sigma_3^2}, \quad x \in \Omega, \quad (2)$$

with the parameter $\mu = (\sigma_1, \sigma_2, \sigma_3)$. This type of source is a special case of the *double ellipsoid source* which was first introduced by Goldak et al. [6] to model the heating effect of a welding torch. We note, however, that the methods developed in this paper are not restricted to the particular welding process considered here, i.e., Gaussian source terms play an important role in many applications in science and engineering — another prominent example is the simulation of airborne contaminants [8, 9, 10]. Furthermore, our approach of course also directly applies to other types of non-affine functions besides Gaussians.

The main task in the analysis and modeling of the welding process is to find parameters μ such that the simulated temperature at one or several measurement points on the surface of the work-piece predicted by (1) and (2) matches the experimental measurements [11]. Given the parameter estimates, we may subsequently aim to control the welding process to achieve a desired weld pool depth [12, 13, 3]. The parameter estimation problem thus needs to be solved in real-time, requiring a rapid and reliable evaluation of the PDE (1).

To achieve this goal we pursue the reduced basis method. The reduced basis method is a model-order reduction technique which provides efficient yet reliable approximations to solutions of parametrized partial differential equations in the many-query or real-time context; see [14] for a recent review of contributions to the methodology. In this paper we focus on parabolic problems with a *non-affine* parameter dependence in the source term — a typical example is given by the Gaussian function (2). To this end we employ the empirical interpolation method (EIM) [15] which serves to construct affine approximations of non-affine parametrized functions. The method is frequently applied in reduced basis approximations of parametrized PDEs with non-affine parameter dependence [15, 16, 17, 18]; the affine approximation of the coefficient function is crucial for computational efficiency.

A posteriori error estimators for non-affine elliptic and parabolic problems have been proposed in [19, 18] and [20], respectively. However, these estimators generally do not provide a rigorous upper bound for the true error due to the contribution of the interpolation error. Only recently, Eftang et al. [21] introduced a rigorous error analysis for the EIM. Furthermore, reduced basis

output approximations and associated output bounds may suffer from a slow convergence, thus requiring a large dimension of the reduced order model to achieve a desired accuracy. To circumvent this problem adjoint procedures were proposed in [22, 23]; however, these previous works only considered *affine* problems. The contributions here are thus (i) rigorous *a posteriori* error bounds for reduced basis approximations of non-affine parabolic problems, and (ii) the development of adjoint procedures for non-affine problems to ensure rapid convergence of the reduced basis output approximation and output error bound.

This paper is organized as follows: in Section 2 we present a short review of the EIM and corresponding rigorous error analysis. The abstract problem formulation and reduced basis approximation for linear coercive parabolic problems with non-affine source terms are introduced in Section 3. In Section 4 we develop our *a posteriori* error estimation procedures and in Section 5 we briefly discuss the sampling technique to generate the reduced basis space. Numerical results for the welding process are presented in Section 6. Finally, we offer concluding remarks in Section 7.

2. Empirical Interpolation Method

In this section we briefly review the EIM and associated *a posteriori* error estimation procedures.

2.1. Coefficient Function Approximation

We assume we are given a function $g: \Omega \times \mathcal{D} \rightarrow \mathbb{R}$ with $g(\cdot; \mu) \in L^\infty(\Omega)$ for all $\mu \in \mathcal{D}$, where $\mathcal{D} \subset \mathbb{R}^P$ is the set of admissible parameters, $\Omega \subset \mathbb{R}^d$, $d = 1, 2, 3$, is a bounded domain, and $L^\infty(\Omega) := \{v \mid \text{ess sup}_{v \in \Omega} |v(x)| < \infty\}$. We introduce a finite but suitably large parameter train sample $\Xi_{\text{train}}^{\text{EIM}} \subset \mathcal{D}$ which shall serve as our surrogate for \mathcal{D} , and a triangulation $\mathcal{T}_{\mathcal{N}}(\Omega)$ of Ω with \mathcal{N} vertices over which we shall in practice realize $g(\cdot; \mu)$ as a piecewise linear function.

The construction of the EIM approximation space W_M^g and set of interpolation points $T_M^g = \{\hat{x}^1, \dots, \hat{x}^M\}$ is based on a greedy algorithm [24]: we first choose $\mu^1 := \arg \max_{\mu \in \Xi_{\text{train}}^{\text{EIM}}} \|g(\cdot; \mu)\|_{L^\infty(\Omega)}$, set $\hat{x}^1 := \arg \text{ess sup}_{x \in \Omega} |g(x; \mu^1)|$, and obtain the first (normalized) EIM basis function $\hat{g}^1(x) := g(x; \mu^1)/g(\hat{x}^1; \mu^1)$. We define $W_1^g := \text{span}\{\hat{g}^1(\cdot)\}$ and introduce the nodal value matrix $G^1 \in \mathbb{R}^{1 \times 1}$ with the single element $G_{1,1}^1 := \hat{g}^1(\hat{x}^1) = 1$.

Then, for $1 \leq M \leq M_{\max} - 1$, we compute the approximation $g_M(\cdot; \mu)$ to $g(\cdot; \mu)$ from

$$g_M(x; \mu) := \sum_{m=1}^M \omega_m(\mu) \hat{g}^m(x), \quad (3)$$

where the coefficient vector $\underline{\omega}(\mu) = [\omega_1(\mu), \dots, \omega_M(\mu)]^T \in \mathbb{R}^M$ is given by the solution of the linear system

$$G^M \underline{\omega}(\mu) = [g(\hat{x}^1; \mu), \dots, g(\hat{x}^M; \mu)]^T. \quad (4)$$

We choose the next parameter

$$\mu_{M+1} := \arg \max_{\mu \in \Xi_{\text{train}}^{\text{EIM}}} \|g(\cdot; \mu) - g_M(\cdot; \mu)\|_{L^\infty(\Omega)} \quad (5)$$

and define the residual $r_M^g(x) := g(x; \mu_{M+1}) - g_M(x; \mu_{M+1})$. The next interpolation point is then set to $\hat{x}^{M+1} := \arg \max_{x \in \Omega} |r_M^g(x)|$, and the next EIM basis function is given by $\hat{g}^{M+1}(x) := r_M^g(x)/r_M^g(\hat{x}^{M+1})$. We define $W_{M+1}^g := \text{span}\{\hat{g}^m(\cdot) \mid 1 \leq m \leq M+1\}$, and update our nodal value matrix $G^{M+1} \in \mathbb{R}^{(M+1) \times (M+1)}$ with components $G_{mn}^{M+1} := \hat{g}^n(\hat{x}^m)$, $1 \leq m, n \leq M+1$. This procedure is either terminated if the maximum dimension of the EIM space M_{\max} is reached or if the maximum of $\|g(\cdot; \mu) - g_M(\cdot; \mu)\|_{L^\infty(\Omega)}$ over all $\mu \in \Xi_{\text{train}}^{\text{EIM}}$ is smaller than some desired tolerance $\varepsilon_{\text{tol}} > 0$. We note that the determination of the coefficients $\underline{\omega}(\mu)$ requires only $\mathcal{O}(M^2)$ computational cost since G^M is lower triangular with unity diagonal and that $\{\hat{g}^m\}_{m=1}^M$ is a basis for W_M^g [15, 16].

Finally, we define a ‘‘Lebesgue constant’’ [25] $\Lambda_M := \sup_{x \in \Omega} \sum_{m=1}^M |V_m^M(x)|$, where $V_m^M(x) \in W_M^g$ are the characteristic functions of W_M^g satisfying $V_m^M(x_n) \equiv \delta_{mn}$, $1 \leq m, n \leq M$; here, δ_{mn} is the Kronecker delta symbol. We recall that (i) the set of all characteristic functions $\{V_m^M\}_{m=1}^M$ is a basis for W_M^g , and (ii) the Lebesgue constant Λ_M satisfies $\Lambda_M \leq 2^M - 1$, see [15, 16]. In applications, the actual asymptotic behavior of Λ_M is much better, as we shall observe subsequently.

2.2. A Posteriori Error Estimation

We briefly recall the non-rigorous and rigorous *a posteriori* error bound procedures for the EIM. Given an approximation $g_M(x; \mu)$ to $g(x; \mu)$, we define the interpolation error as

$$\varepsilon_M^g(\mu) := \|g(\cdot; \mu) - g_M(\cdot; \mu)\|_{L^\infty(\Omega)}. \quad (6)$$

The first error estimator provides a rigorous upper bound for $\varepsilon_M(\mu)$ only under the condition $g(\cdot; \mu) \in W_{M+1}^g$ — thus referred to as ‘‘next-point’’ error bound — whereas the second bound is

rigorous without requiring an additional condition on $g(\cdot; \mu)$. We discuss the trade-off and present numerical results for the performance of both bounds in Section 2.3.

2.2.1. A “Next Point” Error Bound

Assume we are given an approximation $g_M(x; \mu)$ for $M \leq M_{\max} - 1$. If $g(\cdot; \mu) \in W_{M+1}^g$, the interpolation error satisfies [15, 16]

$$\varepsilon_M^g(\mu) = \hat{\varepsilon}_M^g(\mu), \quad (7)$$

where the estimator is defined as $\hat{\varepsilon}_M^g(\mu) := |g(x_{M+1}; \mu) - g_M(x_{M+1}; \mu)|$. We note that the estimator is very inexpensive — it requires only *one additional evaluation* of $g(\cdot; \mu)$ at a single point in Ω . However, in general $g(\cdot; \mu) \notin W_{M+1}^g$, and hence our estimator $\hat{\varepsilon}_M(\mu)$ is indeed a lower bound for the true error, i.e., we have $\varepsilon_M^g(\mu) \geq \hat{\varepsilon}_M^g(\mu)$.

2.2.2. A Rigorous Error Bound

In a recent note, Eftang et al. [21] proposed a new rigorous *a posteriori* error bound which does not rely on the assumption $g(\cdot; \mu) \in W_{M+1}^g$. We shall assume that g is parametrically smooth; for simplicity here, we suppose $g \in C^\infty(\mathcal{D}, L^\infty(\Omega))$.

We first introduce a P -dimensional multi-index $\beta := [\beta_1, \dots, \beta_P]$ with non-negative integers β_1, \dots, β_P . We define the length $|\beta| := \sum_{i=1}^P \beta_i$ and refer to \mathcal{B}_l^P as the set of all multi-indices β of dimension P and length $|\beta| = l$. The number of elements of \mathcal{B}_l^P is then given by $|\mathcal{B}_l^P| = \binom{P+l-1}{l}$. We then define the parametric derivatives

$$g^{(\beta)}(x; \mu) := \frac{\partial^{|\beta|} g(x; \mu)}{\partial \mu_1^{\beta_1} \dots \partial \mu_P^{\beta_P}}. \quad (8)$$

Note that we use the same interpolation space W_M^g for both the function g and its parametric derivatives.

We further assume that for all non-negative integers p there exists a constant $\sigma_p < \infty$ such that $\max_{\mu \in \mathcal{D}} \max_{\beta \in \mathcal{B}_p^P} \|g^{(\beta)}(\cdot; \mu)\|_{L^\infty(\Omega)} \leq \sigma_p$. We also introduce a finite set of points $\Phi \subset \mathcal{D}$ with $|\Phi|$ elements and define $\rho_\Phi := \max_{\mu \in \mathcal{D}} \min_{\phi \in \Phi} \|\mu - \phi\|_2$; here $\|\cdot\|_2$ is the usual Euclidean norm. For given positive integer p , the interpolation error then satisfies [21]

$$\varepsilon_M^g(\mu) \leq \delta_{M,p,\Phi}^g, \quad \forall \mu \in \mathcal{D}, \quad (9)$$

where the error bound is given by

$$\delta_{M,p,\Phi}^g := (1 + \Lambda_M) \frac{\sigma_p}{p!} \rho_\Phi^p P^{p/2} + \sup_{\phi \in \Phi} \left(\sum_{j=0}^{p-1} \frac{\rho_\Phi^j}{j!} P^{j/2} \max_{\beta \in \mathcal{B}_j^P} \left\| g^{(\beta)}(\cdot; \phi) - g_M^{(\beta)}(\cdot; \phi) \right\|_{L^\infty(\Omega)} \right). \quad (10)$$

In practice, higher values of p and larger cardinalities $|\Phi|$ require larger computational effort but result in sharper bounds. However, note that the bound is parameter-independent and can thus be computed *once* offline.

2.3. Numerical Results

In this section we apply the EIM to the *hemispherical volume heat source* defined in (2), given by

$$q(x; \mu) = e^{-x_1^2/\sigma_1^2} e^{-x_2^2/\sigma_2^2} e^{-x_3^2/\sigma_3^2}, \quad x \in \Omega, \quad (11)$$

for $x = (x_1, x_2, x_3) \in \Omega := [-30, 10] \times [0, 10] \times [-10, 0]$ and $\mu = (\sigma_1, \sigma_2, \sigma_3) \in \mathcal{D} := [1.08, 1.32]^3$. The admissible parameter set \mathcal{D} is obtained by taking $\bar{\mu} = [1.2, 1.2, 1.2]$ from the double ellipsoid source of the penetration welding example in [6] and assuming a 10% uncertainty in each parameter. We perform our computations on a triangulation $\mathcal{T}_{\mathcal{N}}(\Omega)$ with $\mathcal{N} = 23891$ vertices (also see Figure 2 for a sketch of the computational domain).

Next, we choose a random parameter train sample $\Xi_{\text{train}}^{\text{EIM}} \subset \mathcal{D}$ with 1000 elements for the greedy algorithm to construct the coefficient-function approximation. For the computation of the rigorous error bound we introduce two deterministic parameter samples $\Phi_1 \subset \mathcal{D}$ and $\Phi_2 \subset \mathcal{D}$ with $|\Phi_1| = 125$ and $|\Phi_2| = 1000$ elements. We shall consider $p = 1, 2, \dots, 5$ and test the rigorous error bound with a random parameter test sample $\Xi_{\text{test}}^{\text{EIM}} \subset \mathcal{D}$ with 100 elements.

In Figures 2.3 (a) and (b), we plot the maximum interpolation error $\varepsilon_M^{q,\max} = \max_{\mu \in \Xi_{\text{test}}^{\text{EIM}}} \varepsilon_M^q(\mu)$ and interpolation error bound $\delta_{M,p,\Phi}^q$ as function of M for $p = 1, 2, \dots, 5$ and $\Phi = \Phi_1$ and $\Phi = \Phi_2$, respectively. We observe that the error bounds initially decrease, but then reach a plateau in M depending on the particular value of p . The plateau itself is due to the fact that the first term in (10) eventually dominates and compromises the sharpness of the bounds. The slight increase of each plateau is related to the growth of the Lebesgue constant Λ_M with M . We note that with increasing p and increasing $|\Phi|$ the bound is sharper for a larger range of M , thus resulting in smaller effectivities.

In Table 1, we first present the Lebesgue constant Λ_M , the condition number $\kappa(G^M)$ of the nodal value matrix G^M , and the maximum interpolation error $\varepsilon_M^{q,\max}$ as a function of M . We

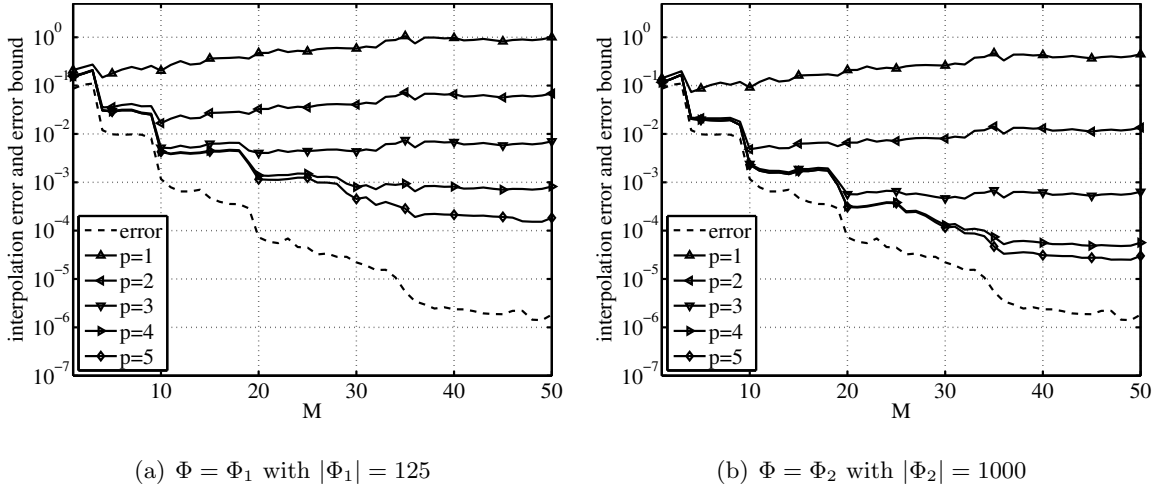


Figure 1: Numerical results for the empirical interpolation of $q(x; \mu)$: maximum interpolation error $\varepsilon_M^{q, \max}$ (dashed line) and interpolation error bound $\delta_{M,p,\Phi}^q$ (solid lines) for $p = 1, \dots, 5$ as a function of M .

observe that the Lebesgue constant grows very slowly, and that the nodal value matrix G^M is quite well-conditioned. Note that the modest growth of the Lebesgue constant is crucial to obtain a sharp error bound [26]. The maximum interpolation error $\varepsilon_M^{q, \max}$ decreases very fast with M .

We next compare the rigorous error bound and the non-rigorous “next-point” error bound. To this end, we also present in Table 1 the rigorous error bound $\delta_{M,p,\Phi}^q$ and the effectivity $\eta_{M,p,\Phi}^q = \delta_{M,p,\Phi}^q / \varepsilon_M^{q, \max}$ for $p = 5$ and $\Phi = \Phi_2$, as well as the maximum non-rigorous error bound $\hat{\varepsilon}_M^{q, \max} = \max_{\mu \in \Xi_{\text{test}}^{\text{EIM}}} \hat{\varepsilon}_M^q(\mu)$ and the average effectivity $\hat{\eta}_M^{q, \text{ave}} = (1/|\Xi_{\text{test}}^{\text{EIM}}|) \sum_{\mu \in \Xi_{\text{test}}^{\text{EIM}}} \hat{\varepsilon}_M^q(\mu) / \varepsilon_M^q(\mu)$. We observe that both the rigorous bound $\delta_{M,p,\Phi}^q$ and the non-rigorous bound $\hat{\varepsilon}_M^{q, \max}$ decrease very fast. However, $\delta_{M,p,\Phi}^q$ is a true upper bound for the interpolation error: the effectivity is always larger than one and — as expected — grows slowly with M (note that $\delta_{M,5,\Phi_2}^q$ reaches the plateau for $M = 36$). The non-rigorous error bound, on the other hand, clearly underestimates the interpolation error: the average effectivities are less than one for all values of M . We recall that the offline stage for the rigorous bound is much more expensive than for the next-point bound [21]. In the online stage, however, the rigorous bound requires no computation at all and the next-point bound requires only one additional evaluation of the non-affine function at a single point in Ω . As long as we can afford the increased offline cost, the rigorous bound is thus clearly preferable.

M	Λ_M	$\kappa(G^M)$	$\varepsilon_M^{q,\max}$	$\delta_{M,5,\Phi_2}^q$	$\eta_{M,5,\Phi_2}^q$	$\hat{\varepsilon}_M^{q,\max}$	$\hat{\eta}_M^{q,\text{ave}}$
10	2.29	4.96	1.17E-03	2.31E-03	1.98	1.13E-03	0.48
20	6.71	7.57	7.30E-05	3.08E-04	4.22	7.30E-05	0.53
30	8.54	13.86	2.20E-05	1.16E-04	5.26	2.20E-05	0.57
40	14.78	22.78	2.36E-06	3.12E-05	13.20	1.97E-06	0.51
50	15.31	25.32	1.83E-06	3.01E-05	16.49	1.22E-06	0.63

Table 1: Numerical results for the empirical interpolation of $q(x;\mu)$: Lebesgue constant Λ_M , condition number $\kappa(G^M)$, maximum interpolation error $\varepsilon_M^{q,\max}$, rigorous error bound $\delta_{M,p,\Phi}^q$ and associated effectivity $\eta_{M,p,\Phi}^q$ for $p = 5$ and $\Phi = \Phi_2$, maximum non-rigorous error bound $\hat{\varepsilon}_M^{q,\max}$ and associated average effectivity $\hat{\eta}_M^{q,\text{ave}}$ as a function of M .

3. Reduced Basis Method

In this section we incorporate the empirical interpolation method described in the last section into our reduced basis approximation to develop an efficient offline-online computational procedure for linear parabolic problems with non-affine source terms.

3.1. Problem Formulation

3.1.1. Abstract Statement

We recall that $\Omega \subset \mathbb{R}^d$, $d = 1, 2, 3$, denotes the spatial domain, a particular point in which is denoted by $x = (x_1, \dots, x_d) \in \Omega$. We also specify the function space $X^e \equiv H_0^1(\Omega)$ — or, more generally $H_0^1(\Omega) \subset X^e \subset H^1(\Omega)$ — where $H^1(\Omega) := \{v \mid v \in L^2(\Omega), \nabla v \in (L^2(\Omega))^d\}$, $H_0^1(\Omega) := \{v \mid v \in H^1(\Omega), v|_{\partial\Omega} = 0\}$, and $L^2(\Omega)$ is the space of square integrable functions over Ω [27].

For simplicity, we will directly consider a time-discrete framework associated to the time interval $I :=]0, t_f]$ ($\bar{I} := [0, t_f]$). We divide \bar{I} into K subintervals of equal length $\Delta t = t_f/K$ and define $t^k := k\Delta t$, $0 \leq k \leq K = t_f/\Delta t$. We shall apply the finite differences θ -method [25] with $0.5 \leq \theta \leq 1$ for the time integration and define $v^{k+\theta} \equiv (1 - \theta)v^k + \theta v^{k+1}$ for any time-discrete variable v^k , $0 \leq k \leq K$. Note that $\theta = 1$ corresponds to the Euler-backward and $\theta = 0.5$ to the Crank-Nicolson scheme.

Our exact problem of interest is then: given a parameter $\mu \in \mathcal{D} \subset \mathbb{R}^P$, we evaluate the output

$$s^e(t^k; \mu) = l(y^e(\cdot, t^k; \mu)), \quad k = 1, \dots, K, \quad (12)$$

where $y^{e,k}(\mu) \equiv y^e(\cdot, t^k; \mu) \in X^e$ satisfies the weak form of the parametrized linear parabolic PDE

$$m(y^{e,k+1}(\mu) - y^{e,k}(\mu), v) + \Delta t a(y^{e,k+\theta}(\mu), v; \mu) = \Delta t f(v; g(\cdot; \mu)) u^{k+\theta} \quad (13)$$

for all $v \in X^e$ and $k = 0, 1, \dots, K-1$, with initial condition (say) $y^e(\cdot, 0; \mu) \equiv 0$ for all $\mu \in \mathcal{D}$. Here, $a(\cdot, \cdot; \mu)$ is an X^e -continuous bilinear form, $m(\cdot, \cdot) = (\cdot, \cdot)_{L^2(\Omega)}$ is a symmetric $L^2(\Omega)$ -continuous bilinear form, $l(\cdot)$ and $f(\cdot; g(\cdot; \mu))$ are $L^2(\Omega)$ -continuous linear forms, $u:]0, t_f] \rightarrow \mathbb{R}$ is the control function, and $g(\cdot; \mu) \in L^\infty(\Omega)$ is a prescribed function which is non-affine with respect to the parameter μ .

We next introduce the X -inner product

$$(v, w)_X = \frac{1}{2} (a(v, w; \bar{\mu}) + a(w, v; \bar{\mu})), \quad \forall v, w \in X^e \quad (14)$$

and induced norm $\|v\|_X = \sqrt{(v, v)_X}$, where $\bar{\mu} \in \mathcal{D}$ is a fixed reference parameter. We also introduce the continuity and coercivity constants of the bilinear form a as

$$\gamma_a^e(\mu) = \sup_{v \in X^e} \sup_{w \in X^e} \frac{a(v, w; \mu)}{\|v\|_X \|w\|_X}, \quad \forall \mu \in \mathcal{D}, \quad (15)$$

and

$$\alpha_a^e(\mu) = \inf_{v \in X^e} \frac{a(v, v; \mu)}{\|v\|_X^2}, \quad \forall \mu \in \mathcal{D}, \quad (16)$$

respectively. Moreover, we assume that the bilinear form a is affine with respect to the parameter μ , i.e.

$$a(\cdot, \cdot; \mu) \equiv \sum_{q=1}^{Q_a} \vartheta_a^q(\mu) a^q(\cdot, \cdot), \quad (17)$$

with parameter-dependent functions $\vartheta_a^q(\mu)$ and parameter-independent bilinear forms a^q .

3.1.2. Truth Approximation

Since we do not have access to the exact semi-discrete solution $y^{e,k}(\mu) \in X^e$ we replace it with a so called ‘‘truth solution’’ $y^k(\mu)$ that resides in a finite element approximation space $X \subset X^e$ of very large dimension \mathcal{N} . Our truth approximation to (12) and (13) is then: given $\mu \in \mathcal{D}$, we evaluate

$$s(t^k; \mu) := l(y^k(\mu)), \quad k = 1, \dots, K, \quad (18)$$

where $y^k(\mu) \in X$ satisfies

$$m(y^{k+1}(\mu) - y^k(\mu), v) + \Delta t a(y^{k+\theta}(\mu), v; \mu) = \Delta t f(v; g(\cdot; \mu)) u^{k+\theta} \quad (19)$$

for all $v \in X$ and $k = 0, 1, \dots, K-1$, with initial condition $y^0(\mu) \equiv 0$. The continuity and coercivity constants of the bilinear form a with respect to X are given by

$$\gamma_a(\mu) = \sup_{v \in X} \sup_{w \in X} \frac{a(v, w; \mu)}{\|v\|_X \|w\|_X}, \quad \forall \mu \in \mathcal{D}, \quad (20)$$

and

$$\alpha_a(\mu) = \inf_{v \in X} \frac{a(v, v; \mu)}{\|v\|_X^2}, \quad \forall \mu \in \mathcal{D}, \quad (21)$$

respectively.

We recall that the affine parameter dependence of the bilinear and linear forms is a crucial ingredient for the computational efficiency, i.e., the offline-online decomposition, of the reduced basis method [16]. We may therefore replace the non-affine function $g(\cdot; \mu)$ in (19) by its affine coefficient-function approximation $g_M(\cdot; \mu)$ defined in (3) to obtain the *approximately* affine problem: find $y_M^k(\mu) \in X$ such that

$$m(y_M^{k+1}(\mu) - y_M^k(\mu), v) + \Delta t a(y_M^{k+\theta}(\mu), v; \mu) = \Delta t f_M(v; \mu) u^{k+\theta} \quad (22)$$

for all $v \in X$ and $k = 0, 1, \dots, K-1$, with $y_M^0(\mu) \equiv 0$; here,

$$f_M(v; \mu) := f(v; g_M(x; \mu)) = f(v; \sum_{q=1}^M \omega_q(\mu) \hat{g}^q(x)) = \sum_{q=1}^M \omega_q(\mu) f(v; \hat{g}^q(x)) = \sum_{q=1}^M \omega_q(\mu) f_M^q(v), \quad (23)$$

for all $v \in X$ and $\mu \in \mathcal{D}$, where the $f_M^q(v) := f(v; \hat{g}^q(x))$, $q = 1, \dots, M$, are parameter-independent linear forms and the $\omega_q(\mu)$, $q = 1, \dots, M$, are calculated from (4). Note that this affine approximation to the truth formulation (19) has only a theoretical purpose. In fact, we stress that $y_M^k(\mu)$ is not computed at any stage in the offline phase and that our *a posteriori* error bounds derived in Section 4 measure the error of the reduced basis approximation with respect to the truth solution $y^k(\mu)$ from (19) and *not* with respect to the affine approximation $y_M^k(\mu)$ to the truth solution. However, since (22) is affine in the parameter we could directly apply the results from [23] at the cost of neglecting the error due to the empirical interpolation [17]. We return to this discussion in Section 4.

To ensure rapid convergence of our reduced basis output approximation we introduce a dual problem [28]. Invoking the LTI property, the truth approximation of the dual of the output at time t^L , $L = 1, \dots, K$, is defined by

$$\psi_L(\cdot, t^k; \mu) = \Psi(\cdot, t^{K-L+k}; \mu), \quad k = 1, \dots, L, \quad (24)$$

where $\Psi^k(\mu) \equiv \Psi(\cdot, t^k; \mu) \in X$ satisfies

$$-m(v, \Psi^{k+1}(\mu) - \Psi^k(\mu)) + \Delta t a(v, \Psi^{k+(1-\theta)}(\mu); \mu) = 0 \quad (25)$$

for all $v \in X$ and $k = 1, \dots, K$, with parameter-independent final condition

$$m(v, \Psi^{K+1}) = l(v) \quad (26)$$

for all $v \in X$. Note that the dual problem inherits the spatial and temporal discretization from the primal problem. Also note that the dual problem is *affine* with respect to the parameter since the source term f does not enter into the dual problem.

3.1.3. Model Problem

The welding process discussed in Section 1 shall serve as our model problem. We consider a coordinate system moving with the (non-dimensional) velocity Pe of the torch in the x_1 -direction; in this coordinate system, the torch is stationary at the origin and the velocity enters as a factor of a convective term in the governing equation, see Figure 2. The temperature y^e in the workpiece is then governed by the convection-diffusion equation (1) with $v = (-Pe, 0, 0)$ and the source term is given by Eq. (2), c.f. [4]. Since our interest is in the non-affine term we keep all parameters fixed except for the ones in the source term; according to the data in [6] we thus set $Pe = 3.65$, $\kappa = 1$, and the control input to $u \equiv 12.3$. We choose the time interval $I =]0, 5]$ with $K = 100$ and $\theta = 1$.

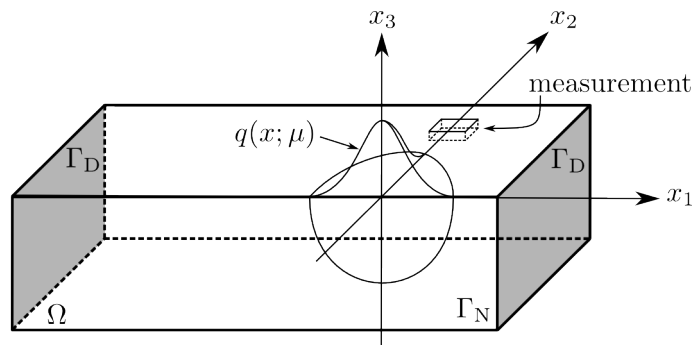


Figure 2: Sketch of the computational domain of the model problem with welding torch at the origin and the measuring point at the top side of the workpiece.

We consider the start-up of the welding process and thus set the initial condition to zero. We assume homogeneous Neumann boundary conditions on Γ_N and homogeneous Dirichlet boundary

conditions on Γ_D , where Γ_D corresponds to the inflow and outflow part of the boundary. The inflow and outflow boundaries are chosen far enough from the origin so as not to influence the temperature at the measurement location.

We next derive the weak formulation of (1) and apply the finite differences θ -method. The governing equation for the temperature $y^k(\mu) \in X$ is thus (19), where X is a linear finite element truth approximation subspace of dimension $\mathcal{N} = 23891$. The bilinear and linear forms are given by $m(w, v) = \int_{\Omega} wv \, dx$, $a(w, v; \mu) = a(w, v) = \int_{\Omega} \nabla w \cdot \nabla v \, dx + \text{Pe} \int_{\Omega} \frac{\partial}{\partial x_1} w v \, dx$, and $f(v; q(\cdot; \mu)) = \int_{\Omega} v q(x; \mu) \, dx$, with $q(x; \mu)$ given by (2). The output of interest is the temperature measurement in a specific volume at the surface, i.e.,

$$s(t^k; \mu) = l(y^k(\mu)) = \frac{1}{|\Omega_m|} \int_{\Omega_m} y^k(\mu) \, dx, \quad k = 1, \dots, K, \quad (27)$$

where $\Omega_m = [-0.25, 0.25] \times [1.5, 2] \times [-0.1, 0]$.

3.2. Reduced Basis Approximation

We suppose that we are given the nested Lagrangian reduced basis spaces

$$X_{N^{\text{pr}}}^{\text{pr}} = \text{span}\{\zeta^{\text{pr},n}(x), 1 \leq n \leq N^{\text{pr}}\}, \quad 1 \leq N^{\text{pr}} \leq N_{\text{max}}^{\text{pr}}, \quad (28)$$

and

$$X_{N^{\text{du}}}^{\text{du}} = \text{span}\{\zeta^{\text{du},n}(x), 1 \leq n \leq N^{\text{du}}\}, \quad 1 \leq N^{\text{du}} \leq N_{\text{max}}^{\text{du}}, \quad (29)$$

where the $\zeta^{\text{pr},n}$, $1 \leq n \leq N^{\text{pr}}$, and the $\zeta^{\text{du},n}$, $1 \leq n \leq N^{\text{du}}$, are mutually $(\cdot, \cdot)_X$ -orthogonal basis functions. In general, we have $N^{\text{pr}} \neq N^{\text{du}}$. We comment on the POD/Greedy algorithm for constructing the basis functions in Section 5.

Our reduced basis approximation $y_{M, N^{\text{pr}}}^k(\mu)$ to $y^k(\mu)$ is obtained by a standard Galerkin projection: given $\mu \in \mathcal{D}$, $y_{M, N^{\text{pr}}}^k(\mu) \in X_{N^{\text{pr}}}^{\text{pr}}$ satisfies

$$m(y_{M, N^{\text{pr}}}^{k+1}(\mu) - y_{M, N^{\text{pr}}}^k(\mu), v) + \Delta t a(y_{M, N^{\text{pr}}}^{k+\theta}(\mu), v; \mu) = \Delta t f_M(v; \mu) u^{k+\theta} \quad (30)$$

for all $v \in X_{N^{\text{pr}}}^{\text{pr}}$ and $k = 0, 1, \dots, K-1$, with initial condition $y_{M, N^{\text{pr}}}^0(\mu) = 0$.

Similarly, we obtain the reduced basis approximation $\Psi_{N^{\text{du}}}^k(\mu) \in X_{N^{\text{du}}}^{\text{du}}$ to $\Psi^k(\mu) \in X$ as solution of

$$-m(v, \Psi_{N^{\text{du}}}^{k+1}(\mu) - \Psi_{N^{\text{du}}}^k(\mu)) + \Delta t a(v, \Psi_{N^{\text{du}}}^{k+(1-\theta)}(\mu); \mu) = 0 \quad (31)$$

for all $v \in X_{N^{\text{du}}}^{\text{du}}$ and $k = 1, \dots, K$, with final condition

$$m(v, \Psi_{N^{\text{du}}}^{K+1}) = l(v) \quad (32)$$

for all $v \in X_{N^{\text{du}}}^{\text{du}}$.

Let $N = (N^{\text{Pr}}, N^{\text{du}})$ be a multi-index indicating the reduced basis dimension of the primal and dual problem respectively. The reduced basis approximation of the output can then be evaluated as

$$s_{M,N}^k(\mu) = l(y_{M,N^{\text{Pr}}}^k(\mu)) + \Delta t \sum_{k'=1}^k r_{N^{\text{Pr}}}^{y,k'}(\Psi_{N^{\text{du}}}^{K-k+k'+(1-\theta)}(\mu); \mu), \quad (33)$$

for $k = 1, \dots, K$; here, the residual of the primal problem is defined as

$$r_{N^{\text{Pr}}}^{y,k}(v; \mu) := f_M(v; \mu) u^{k-1+\theta} - a(y_{M,N^{\text{Pr}}}^{k-1+\theta}(\mu), v; \mu) - \frac{1}{\Delta t} m(y_{M,N^{\text{Pr}}}^k(\mu) - y_{M,N^{\text{Pr}}}^{k-1}(\mu), v), \quad (34)$$

with $k = 1, \dots, K$ for all $v \in X$. We may also obtain a simple reduced basis output approximation from

$$\tilde{s}_{M,N^{\text{Pr}}}^k(\mu) = l(y_{M,N^{\text{Pr}}}^k(\mu)), \quad (35)$$

$k = 1, \dots, K$. Note that we do not require the dual problem to evaluate $\tilde{s}_{M,N^{\text{Pr}}}^k(\mu)$. We shall compare the performance of both output approximations in Section 6.

3.3. Computational Procedure

Now we develop the offline-online computational procedure in order to fully exploit the dimension reduction. First, we express $y_{M,N^{\text{Pr}}}^k(\mu)$ in the form

$$y_{M,N^{\text{Pr}}}^k(\mu) = \sum_{i=1}^{N^{\text{Pr}}} \left(y_{M,N^{\text{Pr}}}^k(\mu) \right)_i \zeta^{\text{Pr},i} \quad (36)$$

and choose as test functions $v = \zeta^{\text{Pr},i}(x)$, $1 \leq i \leq N^{\text{Pr}}$ in Eq. (30). We thus obtain

$$\begin{aligned} & \sum_{i=1}^{N^{\text{Pr}}} \left(\left(y_{M,N^{\text{Pr}}}^{k+1}(\mu) \right)_i - \left(y_{M,N^{\text{Pr}}}^k(\mu) \right)_i \right) m(\zeta^{\text{Pr},i}, \zeta^{\text{Pr},j}; \mu) \\ & + \Delta t \sum_{i=1}^{N^{\text{Pr}}} \left(y_{M,N^{\text{Pr}}}^{k+\theta}(\mu) \right)_i a(\zeta^{\text{Pr},i}, \zeta^{\text{Pr},j}; \mu) = \Delta t f_M(\zeta^{\text{Pr},j}; \mu) u^{k+\theta} \end{aligned} \quad (37)$$

for all $j = 1, \dots, N^{\text{Pr}}$ and $k = 0, 1, \dots, K-1$, which we can rewrite in the algebraic form

$$\begin{aligned} (M^{\text{Pr}} + \theta \Delta t A^{\text{Pr}}(\mu))^{\text{T}} \underline{y}_{M,N^{\text{Pr}}}^{k+1}(\mu) &= (M^{\text{Pr}} - (1-\theta) \Delta t A^{\text{Pr}}(\mu))^{\text{T}} \underline{y}_{M,N^{\text{Pr}}}^k(\mu) \\ &+ \Delta t \left((1-\theta) u^k + \theta u^{k+1} \right) F_M^{\text{Pr}}(\mu), \end{aligned} \quad (38)$$

for $k = 0, 1, \dots, K - 1$, where

$$A^{\text{Pr}}(\mu) = \left[A_{ij}^{\text{Pr}}(\mu) \right] \in \mathbb{R}^{N^{\text{Pr}} \times N^{\text{Pr}}}, \quad A_{ij}^{\text{Pr}}(\mu) = a(\zeta^{\text{Pr},i}, \zeta^{\text{Pr},j}; \mu), \quad 1 \leq i, j \leq N^{\text{Pr}} \quad (39)$$

$$M^{\text{Pr}} = \left[M_{ij}^{\text{Pr}} \right] \in \mathbb{R}^{N^{\text{Pr}} \times N^{\text{Pr}}}, \quad M_{ij}^{\text{Pr}} = m(\zeta^{\text{Pr},i}, \zeta^{\text{Pr},j}), \quad 1 \leq i, j \leq N^{\text{Pr}} \quad (40)$$

$$F_M^{\text{Pr}}(\mu) = \left[F_{M,j}^{\text{Pr}}(\mu) \right] \in \mathbb{R}^{N^{\text{Pr}}}, \quad F_{M,j}^{\text{Pr}}(\mu) = f_M(\zeta^{\text{Pr},j}; \mu), \quad 1 \leq j \leq N^{\text{Pr}} \quad (41)$$

and $\underline{y}_{M,N^{\text{Pr}}}^k(\mu) = \left[\left(y_{M,N^{\text{Pr}}}^k(\mu) \right)_1, \dots, \left(y_{M,N^{\text{Pr}}}^k(\mu) \right)_{N^{\text{Pr}}} \right]^{\text{T}} \in \mathbb{R}^{N^{\text{Pr}}}$. The initial condition is given by $\underline{y}_{M,N^{\text{Pr}}}^0(\mu) = \underline{0}$.

We now invoke the affine parameter dependence (17) to obtain

$$A^{\text{Pr}}(\mu) = \sum_{q=1}^{Q_a} \vartheta_a^q(\mu) A^{\text{Pr},q}, \quad (42)$$

where the parameter independent matrices $A^{\text{Pr},q} = \left[A_{ij}^{\text{Pr},q} \right] \in \mathbb{R}^{N^{\text{Pr}} \times N^{\text{Pr}}}$, $1 \leq q \leq Q_a$, are given by $A_{ij}^{\text{Pr},q} = a^q(\zeta^{\text{Pr},i}, \zeta^{\text{Pr},j})$, $1 \leq i, j \leq N^{\text{Pr}}$, $1 \leq q \leq Q_a$. Furthermore, it follows from (23) that we can express $F_M^{\text{Pr}}(\mu)$ as

$$F_M^{\text{Pr}}(\mu) = \sum_{q=1}^M \omega_q(\mu) F_M^{\text{Pr},q}, \quad (43)$$

where the parameter independent vectors $F_M^{\text{Pr},q} = \left[F_{M,j}^{\text{Pr},q} \right] \in \mathbb{R}^{N^{\text{Pr}}}$, $1 \leq q \leq M$, are given by $F_{M,j}^{\text{Pr},q} = f_M^q(\zeta^{\text{Pr},j}) = f(\zeta^{\text{Pr},j}; \hat{g}^q(x))$, $1 \leq j \leq N^{\text{Pr}}$, $1 \leq q \leq M$, and the $\omega_q(\mu)$, $1 \leq q \leq M$, are calculated from (4). The computational procedure for the dual problem and the output approximation directly follows from the primal problem and is therefore omitted [23].

The offline-online decomposition is now clear. In the offline stage — performed only once — we compute the basis functions $\zeta^{\text{Pr},1}(x), \dots, \zeta^{\text{Pr},N^{\text{Pr}}}(x)$ of the primal and $\zeta^{\text{du},1}(x), \dots, \zeta^{\text{du},N^{\text{du}}}(x)$ of the dual problem. Then we determine the parameter-independent matrices $A^{\text{Pr},q}$, M^{Pr} , and $F_M^{\text{Pr},q}$ for the primal problem; $A^{\text{du},q}$ and M^{du} for the dual problem; and $A^{\text{Pr,du},q}$, $M^{\text{Pr,du}}$, $F_M^{\text{du},q}$, and L^{Pr} for the output approximation. The computational costs are thus $\mathcal{O}(K + (N^{\text{Pr}} + N^{\text{du}}))$ solutions of the \mathcal{N} -dimensional truth finite element approximation and $\mathcal{O}(Q_a((N^{\text{Pr}})^2 + (N^{\text{du}})^2 + N^{\text{Pr}}N^{\text{du}}) + M(N^{\text{Pr}}N^{\text{du}}))$ \mathcal{N} -inner products. The storage requirements are $\mathcal{O}(Q_a((N^{\text{Pr}})^2 + (N^{\text{du}})^2 + N^{\text{Pr}}N^{\text{du}}) + M(N^{\text{Pr}} + N^{\text{du}}))$.

In the online stage — performed many times, for each new parameter value μ — we assemble the parameter-dependent matrices $A^{\text{Pr}}(\mu)$, $A^{\text{du}}(\mu)$, $A^{\text{Pr,du}}(\mu)$ and vectors $F_M^{\text{Pr}}(\mu)$, $F_M^{\text{du}}(\mu)$ which requires $\mathcal{O}(Q_a((N^{\text{Pr}})^2 + (N^{\text{du}})^2 + N^{\text{Pr}}N^{\text{du}}) + M^2 + M(N^{\text{Pr}} + N^{\text{du}}))$. We then solve the primal

problem (38) and the dual problem — considering the LTI property and the fact that the matrices are generally full — at cost $\mathcal{O}((N^{\text{pr}})^3 + (N^{\text{du}})^3 + K((N^{\text{pr}})^2 + (N^{\text{du}})^2))$. Finally, the evaluation of the output approximation (33) at time t^k requires $\mathcal{O}(kN^{\text{pr}}N^{\text{du}})$ — the evaluation of the output for all K timesteps has a cost of $\mathcal{O}(K^2N^{\text{pr}}N^{\text{du}})$ due to the residual correction term. However, evaluating the simple reduced basis output approximation (35) at all timesteps costs only $\mathcal{O}(KN^{\text{pr}})$. The online stage is thus independent of the truth finite element dimension \mathcal{N} .

4. *A Posteriori* Error Estimation

In this section we develop rigorous *a posteriori* error bounds for the reduced basis approximation of the state and output. The new ingredients are (i) the combination of the rigorous error bounds for the EIM of Section 2 with the “standard” affine reduced basis error bounds, and (ii) the development of adjoint procedures for non-affine parabolic problems. We recall that *non-rigorous* error bounds have been developed for elliptic and parabolic problems in [19, 18] and [20], respectively; and that adjoint procedures for *affine* parabolic problems have been proposed in [23]. Furthermore, we refer the interested reader to [16] for *a priori* convergence results of non-affine problems.

4.1. Preliminaries

To begin, we assume that we are given a positive lower bound for the coercivity constant $\alpha_a(\mu)$: $\alpha_a^{\text{LB}}(\mu) : \mathcal{D} \rightarrow \mathbb{R}_+$ satisfies

$$\alpha_a(\mu) \geq \alpha_a^{\text{LB}}(\mu) \geq \alpha_a^0 > 0, \quad \forall \mu \in \mathcal{D}. \quad (44)$$

This bound can be calculated using the Successive Constraint Method (SCM) [29]; however, simpler recipes often suffice [30, 31]. We next introduce the dual norm of the primal residual (34), given by

$$\left\| r_{N^{\text{pr}}}^{y,k}(\cdot; \mu) \right\|_{X^*} = \sup_{v \in X} \frac{r_{N^{\text{pr}}}^{y,k}(v; \mu)}{\|v\|_X}, \quad 1 \leq k \leq K, \quad (45)$$

and the dual norm of the dual residual

$$\left\| r_{N^{\text{du}}}^{\Psi,k}(\cdot; \mu) \right\|_{X^*} = \sup_{v \in X} \frac{r_{N^{\text{du}}}^{\Psi,k}(v; \mu)}{\|v\|_X}, \quad 1 \leq k \leq K, \quad (46)$$

where

$$r_{N^{\text{du}}}^{\Psi,k}(v; \mu) := -a(v, \Psi_{N^{\text{du}}}^{k+(1-\theta)}(\mu); \mu) + \frac{1}{\Delta t} m(v, \Psi_{N^{\text{du}}}^{k+1}(\mu) - \Psi_{N^{\text{du}}}^k(\mu)), \quad (47)$$

for $v \in X$, $1 \leq k \leq K$. Finally, the spatio-temporal energy norm for the primal problem is defined as

$$\left\| \|v^k\|_{\mu}^{\text{Pr}} \right\| := \left(m(v^k, v^k) + \Delta t \sum_{k'=1}^k a(v^{k'-1+\theta}, v^{k'-1+\theta}; \mu) \right)^{\frac{1}{2}}, \quad (48)$$

and for the dual problem as

$$\left\| \|v^k\|_{\mu}^{\text{du}} \right\| := \left(m(v^k, v^k) + \Delta t \sum_{k'=k}^K a(v^{k+(1-\theta)}, v^{k+(1-\theta)}; \mu) \right)^{\frac{1}{2}}. \quad (49)$$

4.2. Primal Variable

We first revisit our discussion related to the truth formulation (19) and its affine approximation (22). Assuming we are interested in the error between the reduced basis approximation, $y_{M, N^{\text{Pr}}}^k(\mu)$, and the affine approximation to the truth, $y_M^k(\mu)$, we can directly apply the result from [23]. Indeed, the error, $y_M^k(\mu) - y_{M, N^{\text{Pr}}}^k(\mu)$, satisfies

$$\left\| \|y_M^k(\mu) - y_{M, N^{\text{Pr}}}^k(\mu)\|_{\mu}^{\text{Pr}} \right\| \leq \Delta_{N^{\text{Pr}}}^{y_M, k}(\mu), \quad \forall \mu \in \mathcal{D}, \forall k = 1, \dots, K, \quad (50)$$

where the error bound is given by

$$\Delta_{N^{\text{Pr}}}^{y_M, k}(\mu) := \left(\frac{\Delta t}{\alpha_a^{\text{LB}}(\mu)} \sum_{k'=1}^k \left\| r_{N^{\text{Pr}}}^{y, k'}(\cdot; \mu) \right\|_{X^*}^2 \right)^{\frac{1}{2}}. \quad (51)$$

Although this approach is appealing due to its simplicity, the error bound (51) *does not* account for the error due to the empirical interpolation of the non-affine terms. Our goal is to incorporate the interpolation error into the bound formulation and thus provide a rigorous upper bound for the error between the reduced basis, $y_{M, N^{\text{Pr}}}^k(\mu)$, and the truth approximation, $y^k(\mu)$. However, we shall use the bound defined in (51) for notational convenience and to show the analogy between the affine and non-affine error bound formulations.

We are now ready to state

Proposition 1. *Let $\mathcal{P} = (p, \Phi)$ be a multi-index with a positive integer p and a finite subset Φ of \mathcal{D} . Then the error*

$$e_{M, N^{\text{Pr}}}^{y, k}(\mu) \equiv y^k(\mu) - y_{M, N^{\text{Pr}}}^k(\mu) \quad (52)$$

of the reduced basis solution $y_{M, N^{\text{Pr}}}^k(\mu)$ with respect to the truth solution $y^k(\mu)$ satisfies

$$\left\| \|e_{M, N^{\text{Pr}}}^{y, k}(\mu)\|_{\mu}^{\text{Pr}} \right\| \leq \Delta_{M, N^{\text{Pr}}, \mathcal{P}}^{y, k}(\mu), \quad \forall \mu \in \mathcal{D}, \forall k = 1, \dots, K, \quad (53)$$

where the error bound $\Delta_{M,N^{\text{Pr}},\mathcal{P}}^{y,k}(\mu)$ is defined by

$$\Delta_{M,N^{\text{Pr}},\mathcal{P}}^{y,k}(\mu) := \left(2 \left(\Delta_{N^{\text{Pr}}}^{y_M,k}(\mu) \right)^2 + \frac{2\Delta t}{\alpha_a^{\text{LB}}(\mu)} \left(\delta_{M,p,\Phi}^g \|f(\cdot; 1)\|_{X^*} \right)^2 \sum_{k'=1}^k \left(u^{k-1+\theta} \right)^2 \right)^{\frac{1}{2}} \quad (54)$$

and $\Delta_{N^{\text{Pr}}}^{y_M,k}(\mu)$ is defined in (51) and $\|f(\cdot; 1)\|_{X^*} := \sup_{v \in X} \frac{f(v; 1)}{\|v\|_X}$.

We note that the error bound (54) consists of two terms: the first term contains the error bound defined in (51) and thus represents the contribution due to the affine terms; the second term depends on the estimator $\delta_{M,p,\Phi}^g$ for the interpolation error, and thus accounts for the error due to the non-affine function interpolation.

Proof. The proof is an extension of the one presented in [23] for affine problems with the added complexity due to error in the function interpolation. Following the same steps, we obtain

$$\begin{aligned} m(e_{M,N^{\text{Pr}}}^{y,k}, e_{M,N^{\text{Pr}}}^{y,k}) - m(e_{M,N^{\text{Pr}}}^{y,k-1}, e_{M,N^{\text{Pr}}}^{y,k-1}) + 2\Delta t a(e_{M,N^{\text{Pr}}}^{y,k-1+\theta}, e_{M,N^{\text{Pr}}}^{y,k-1+\theta}; \mu) \\ \leq 2\Delta t r_{N^{\text{Pr}}}^{y,k}(e_{M,N^{\text{Pr}}}^{y,k-1+\theta}; \mu) + 2\Delta t f(e_{M,N^{\text{Pr}}}^{y,k-1+\theta}, g(\mu) - g_M(\mu)) u^{k-1+\theta}. \end{aligned} \quad (55)$$

The new ingredient is the non-affine contribution on the right hand side. Using Young's inequality, the first term on the right hand side can be bounded by

$$r_{N^{\text{Pr}}}^{y,k}(e_{M,N^{\text{Pr}}}^{y,k-1+\theta}; \mu) \leq \frac{1}{2} \left(\frac{2}{\alpha_a^{\text{LB}}(\mu)} \left\| r_{N^{\text{Pr}}}^{y,k}(\cdot; \mu) \right\|_{X^*}^2 + \frac{\alpha_a^{\text{LB}}(\mu)}{2} \left\| e_{M,N^{\text{Pr}}}^{y,k-1+\theta} \right\|_X^2 \right). \quad (56)$$

We now use the EIM rigorous bound result (9), (10), and Young's inequality to bound the second term on the right hand side by

$$\begin{aligned} f(e_{M,N^{\text{Pr}}}^{y,k-1+\theta}, g(\mu) - g_M(\mu)) u^{k-1+\theta} \\ \leq \frac{1}{2} \left(\frac{\alpha_a^{\text{LB}}(\mu)}{2} \left\| e_{M,N^{\text{Pr}}}^{y,k-1+\theta} \right\|_X^2 + \frac{2}{\alpha_a^{\text{LB}}(\mu)} \left(\delta_{M,p,\Phi}^g \|f(\cdot; 1)\|_{X^*} u^{k-1+\theta} \right)^2 \right). \end{aligned} \quad (57)$$

The desired result then directly follows from (55), (56), (57), the coercivity of a and (44) after summing from $k' = 1$ to k .

□

4.3. Dual Variable

Since the dual problem is affinely parameter dependent, the results from [23] directly apply: the error

$$e_{N^{\text{du}}}^{\Psi,k}(\mu) \equiv \Psi^k(\mu) - \Psi_{N^{\text{du}}}^k(\mu) \quad (58)$$

in the dual state satisfies

$$\left\| e_{N^{\text{du}}}^{\Psi,k}(\mu) \right\|_{\mu}^{\text{du}} \leq \Delta_{N^{\text{du}}}^{\Psi,k}(\mu) \quad \forall \mu \in \mathcal{D}, \forall k = 1, \dots, K, \quad (59)$$

where the dual state error bound is given by

$$\Delta_{N^{\text{du}}}^{\Psi,k}(\mu) := \left(\frac{\Delta t}{\alpha_a^{\text{LB}}(\mu)} \sum_{k'=k}^K \left\| r_{N^{\text{du}}}^{\Psi,k'}(\cdot; \mu) \right\|_{X^*}^2 \right)^{\frac{1}{2}}. \quad (60)$$

4.4. Output Bounds

Finally, the error bound for the output approximation is given in the following proposition. We provide the proof in Appendix A.

Proposition 2. *Let $\mathcal{P} = (p, \Phi)$ be a multi-index with a positive integer p and a finite subset Φ of \mathcal{D} . The error between the truth output $s^k(\mu)$ and its reduced basis approximation $s_{M,N}^k(\mu)$ satisfies*

$$\left| s^k(\mu) - s_{M,N}^k(\mu) \right| \leq \Delta_{M,N,\mathcal{P}}^{s,k}(\mu) \quad \forall \mu \in \mathcal{D}, \forall k = 1, \dots, K, \quad (61)$$

with the primal-dual output error bound

$$\begin{aligned} \Delta_{M,N,\mathcal{P}}^{s,k}(\mu) &:= \Delta_{N^{\text{pr}}}^{y_{M,k}}(\mu) \Delta_{N^{\text{du}}}^{\Psi,K-k+1}(\mu) \\ &\quad + \delta_{M,p,\Phi}^g \Delta_{N^{\text{du}}}^{\Psi,K-k+1}(\mu) \|f(\cdot; 1)\|_{X^*} \left(\frac{\Delta t}{\alpha_a^{\text{LB}}(\mu)} \sum_{k'=1}^k \left(u^{k'-1+\theta} \right)^2 \right)^{\frac{1}{2}} \\ &\quad + \Delta t \delta_{M,p,\Phi}^g \sum_{k'=1}^k \left| f(\Psi_{N^{\text{du}}}^{K-k+k'+(1-\theta)}(\mu); 1) u^{k'-1+\theta} \right|, \end{aligned} \quad (62)$$

where $\Delta_{N^{\text{pr}}}^{y_{M,k}}(\mu)$ and $\Delta_{N^{\text{du}}}^{\Psi,k}(\mu)$ are defined in (51) and (60), respectively.

We also introduce a simple reduced basis output approximation and corresponding error bound which shall serve as a comparison for the primal-dual formulation.

Proposition 3. *Let $\mathcal{P} = (p, \Phi)$ be a multi-index with a positive integer p and a finite subset Φ of \mathcal{D} . The error between the truth output $s^k(\mu)$ and its simple reduced basis approximation $\tilde{s}_{M,N^{\text{pr}}}^k(\mu)$ satisfies*

$$\left| s^k(\mu) - \tilde{s}_{M,N^{\text{pr}}}^k(\mu) \right| \leq \tilde{\Delta}_{M,N^{\text{pr}},\mathcal{P}}^{s,k}(\mu) \quad \forall \mu \in \mathcal{D}, \forall k = 1, \dots, K, \quad (63)$$

with the simple output error bound

$$\tilde{\Delta}_{M,N^{\text{pr}},\mathcal{P}}^{s,k}(\mu) := \sup_{v \in X} \frac{l(v)}{\|v\|_{L^2(\Omega)}} \Delta_{M,N^{\text{pr}},\mathcal{P}}^{y,k}(\mu). \quad (64)$$

Proof. From the definition of the simple output we obtain

$$\left| s^k(\mu) - \tilde{s}_{M,N^{\text{Pr}}}^k(\mu) \right| = \left| l(e_{M,N^{\text{Pr}}}^{y,k}(\mu)) \right| = \sup_{v \in X} \frac{l(v)}{\|v\|_{L^2(\Omega)}} \left\| e_{M,N^{\text{Pr}}}^{y,k}(\mu) \right\|_{L^2(\Omega)}. \quad (65)$$

The result directly follows since

$$\left\| e_{M,N^{\text{Pr}}}^{y,k}(\mu) \right\|_{L^2(\Omega)} = \left(m(e_{M,N^{\text{Pr}}}^{y,k}(\mu), e_{M,N^{\text{Pr}}}^{y,k}(\mu)) \right)^{\frac{1}{2}} \leq \left\| e_{M,N^{\text{Pr}}}^{y,k}(\mu) \right\|_{\mu}^{\text{Pr}}. \quad (66)$$

for all $\mu \in \mathcal{D}$. \square

At this point, we make several comments from a theoretical point of view. First, similar to the error bound for the primal variable, the output error bound (62) consists of several terms: the first term represents the usual primal-dual contribution to the error bound. If the problem becomes affine, i.e., we redefine the affine approximation to the truth finite element approximation given by (22) to be our new “truth” the error bound then simplifies to the one proposed for affine problems in [23]: the interpolation error bound $\delta_{M,p,\Phi}^g$ vanishes and only the primal-dual contribution in the first term, $\Delta_{N^{\text{Pr}}}^{y_M,k}(\mu) \Delta_{N^{\text{du}}}^{\Psi,K-k+1}(\mu)$, remains. However, for non-affine problems we obtain two additional terms which account for the error due to the function approximation.

Second, the goal of the adjoint formulation is to recover the square effect, i.e., a primal contribution multiplied by a dual contribution, in the output bound. The second term of the output error bound (62) also shows this square effect since the error bound of the dual state is multiplied with the EIM error bound. The last term, on the other side, only contains the EIM error bound $\delta_{M,p,\Phi}^g$. We thus need to choose M large enough — and thus guarantee that $\delta_{M,p,\Phi}^g$ is small enough — so that the last term does not limit the convergence of the overall output error bound.

Third, we observe that the simple output error bound does not show the square effect. We thus expect a much slower convergence of the output bound for the primal-only formulation.

4.5. Computational Procedure

The offline-online computational procedures for the calculation of the error bounds $\Delta_{M,N^{\text{Pr}},\mathcal{P}}^{y,k}(\mu)$, $\tilde{\Delta}_{M,N^{\text{Pr}},\mathcal{P}}^{s,k}(\mu)$ and $\Delta_{M,N,\mathcal{P}}^{s,k}(\mu)$ are a direct extension of the procedures described in [23, 20]. We therefore omit the details and only summarize the computational costs involved in the online stage.

We recall that the EIM *a posteriori* error bound $\delta_{M,p,\Phi}^g$ is evaluated offline and does not require any online calculations. In the online stage the computational cost to evaluate $\Delta_{M,N^{\text{Pr}},\mathcal{P}}^{y,k}(\mu)$ and $\tilde{\Delta}_{M,N^{\text{Pr}},\mathcal{P}}^{s,k}(\mu)$ for all K is thus $\mathcal{O}(K(N^{\text{Pr}}MQ_a + (N^{\text{Pr}})^2Q_a^2))$, while the computational cost to evaluate the primal-dual output bound $\Delta_{M,N,\mathcal{P}}^{s,k}(\mu)$ is $\mathcal{O}(K(N^{\text{Pr}}MQ_a + (N^{\text{Pr}})^2Q_a^2 + (N^{\text{du}})^2Q_a^2))$.

5. Sampling Procedure

In this section we review the combined proper orthogonal decomposition (POD) and greedy sampling procedure [32] to construct the primal and dual reduced basis space.

We only summarize the POD/Greedy procedure for the primal problem: we first choose an arbitrary parameter value $\mu_1 \in \mathcal{D}$ and set $S_0 = \{0\}$, $X_0 = \{0\}$, $N^{\text{Pr}} = 0$. Then, for $1 \leq N^{\text{Pr}} \leq N_{\text{max}}^{\text{Pr}}$, we first set the parameter sample to $S_{N^{\text{Pr}}} = S_{N^{\text{Pr}}-1} \cup \{\mu_{N^{\text{Pr}}}\}$ and compute the projection error $e_{N^{\text{Pr}}, \text{proj}}^{y,k}(\mu_{N^{\text{Pr}}})$, $k = 1, \dots, K$, which is the difference of the truth solution $y^k(\mu_{N^{\text{Pr}}})$ and its X -orthogonal projection $y_{\text{proj}}^k(\mu_{N^{\text{Pr}}})$ onto the reduced basis space $X_{N^{\text{Pr}}}$. We then expand the reduced basis space by the largest POD mode of the time history of $\{e_{N^{\text{Pr}}, \text{proj}}^{y,k}(\mu_{N^{\text{Pr}}}) \mid 1 \leq k \leq K\}$ which we compute using the method of snapshots [33]. Finally, we choose the next parameter value from $\mu_{N^{\text{Pr}}+1} = \arg \max_{\mu \in \Xi_{\text{train}}} \Delta_{M, N^{\text{Pr}}}^{y,K}(\mu) / \|\|y_{M, N^{\text{Pr}}}^K(\mu)\|\|_{\mu}^{\text{Pr}}$, i.e. we perform a greedy search over Ξ_{train} for the largest relative *a posteriori* state error bound at the final time. Here $\Xi_{\text{train}} \subset \mathcal{D}$ denotes a finite but suitably large parameter train sample.

Note that we set $M = M_{\text{max}}$ during the greedy procedure so that the contribution of the non-affine terms does not spoil the greedy search. If the control $u(t^k)$ is not known in advance, e.g., in an (optimal) control setting, we may perform the sampling procedure with the impulse input $\delta^{1,k}$ without detriment to the accuracy of the resulting reduced basis approximation [23].

6. Numerical Results

We now present numerical results for our model problem introduced in Section 3.1.3. The generation of the EIM approximation of the non-affine source term and the numerical results are discussed in Section 2.3.

We first choose a random parameter sample $\Xi_{\text{train}} \subset \mathcal{D}$ with 1000 elements to construct the primal reduced basis space $X_{N^{\text{Pr}}}^{\text{Pr}}$ according to the POD/Greedy sampling procedure in Section 5. Since the dual problem is parameter-independent we perform only the POD part of the POD/Greedy procedure to construct the dual reduced basis space $X_{N^{\text{du}}}^{\text{du}}$. For the numerical tests we use a random parameter test sample $\Xi_{\text{test}} \subset \mathcal{D}$ with 60 elements.

In Figure 3 we plot, as a function of N^{Pr} and M , the maximum relative state error bound $\Delta_{M, N^{\text{Pr}}, \mathcal{P}}^{y, \text{max, rel}} = \max_{\mu \in \Xi_{\text{test}}} \Delta_{M, N^{\text{Pr}}, \mathcal{P}}^{y,K}(\mu) / \|\|y^K(\mu)\|\|_{\mu}^{\text{Pr}}$ of the primal problem at the final time step t^K . For the interpolation error bound we used $p = 5$ and $\Phi = \Phi_2$. We observe that the reduced

basis approximation converges quite rapidly. We also note that the curves for fixed M stagnate at some point and that the curves level off at smaller values as M increases: for fixed M the EIM error bound will ultimately dominate for large N^{Pr} ; increasing M renders the coefficient function approximation more accurate, which in turn leads to a drop in the error. The separation points of the N^{Pr} - M -convergence curves reflect a balanced contribution of both error bound terms in (54); neither N^{Pr} nor M limit the convergence of the reduced basis approximation.

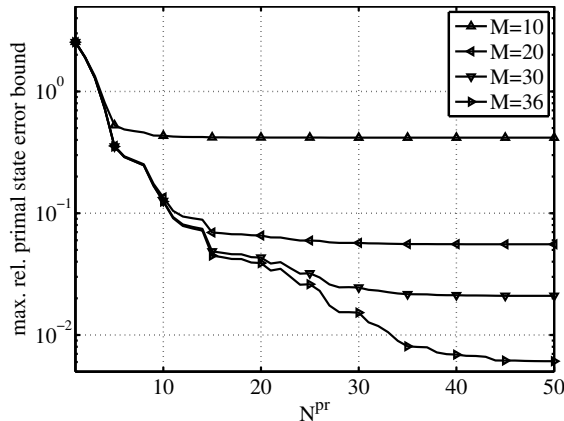


Figure 3: Numerical results for the reduced basis method: maximum relative primal state error bound $\Delta_{M,N^{\text{Pr}},\mathcal{P}}^{y,\text{max,rel}}$ as a function of N^{Pr} for $M = 10, 20, 30, 36$, $p = 5$ and $\Phi = \Phi_2$.

In Table 2 we present, as a function of N^{Pr} and M , the maximum relative truth error $\varepsilon_{M,N^{\text{Pr}}}^{y,\text{max,rel}}$, the maximum relative error bound $\Delta_{M,N^{\text{Pr}},\mathcal{P}}^{y,\text{max,rel}}$, and the average effectivity $\eta_{M,N^{\text{Pr}},\mathcal{P}}^{y,\text{ave}}$; here, $\varepsilon_{M,N^{\text{Pr}}}^{y,\text{max,rel}}$ is the maximum over Ξ_{test} of $\varepsilon_{M,N^{\text{Pr}}}^{y,K}(\mu) / \|\|y^K(\mu)\|\|_{\mu}^{\text{Pr}}$, and $\eta_{M,N^{\text{Pr}},\mathcal{P}}^{y,\text{ave}}$ is the average over Ξ_{test} of $\Delta_{M,N^{\text{Pr}},\mathcal{P}}^{y,K}(\mu) / \varepsilon_{M,N^{\text{Pr}}}^{y,K}(\mu)$. Note that the tabulated (N^{Pr}, M) values correspond roughly to the separation points of the N^{Pr} - M -convergence curves. We observe that the effectivities are larger than but close to 1; we obtain rigorous and sharp upper bounds for the true error.

The corresponding results for the dual problem are presented in Table 3. Since the dual is parameter-independent, we observe a much faster convergence of the error and the error bound than for the primal problem. The effectivities are thus very good for all values of N^{du} .

We next turn to the output error bound and present in Figure 4 the maximum relative primal-dual output error bound $\Delta_{M,N,\mathcal{P}}^{s,\text{max,rel}} = \max_{\mu \in \Xi_{\text{test}}} \Delta_{M,N,\mathcal{P}}^{s,K}(\mu)$ at the final time step t^K as a function of N^{Pr} for $N^{\text{du}} = 5, 10, 15, 20$. We use $p = 5$, $\Phi = \Phi_2$ and $M = 36$ for the empirical interpolation. The convergence curves show the full potential and advantage of the primal-dual formulation for

N^{pr}	M	$\varepsilon_{M,N^{\text{pr}}}^{y,\text{max,rel}}$	$\Delta_{M,N^{\text{pr}},\mathcal{P}}^{y,\text{max,rel}}$	$\eta_{M,N^{\text{pr}},\mathcal{P}}^{y,\text{ave}}$
5	10	9.88E-02	5.28E-01	6.57
10	20	3.76E-02	1.35E-01	4.19
25	30	7.59E-03	3.21E-02	5.56
40	36	1.02E-03	6.89E-03	7.88

Table 2: Reduced basis approximation of the primal state: maximum relative truth error $\varepsilon_{M,N^{\text{pr}}}^{y,\text{max,rel}}$, maximum relative error bound $\Delta_{M,N^{\text{pr}},\mathcal{P}}^{y,\text{max,rel}}$ and average effectivity $\eta_{M,N^{\text{pr}},\mathcal{P}}^{y,\text{ave}}$ as a function of M and N^{pr} . The values of the error bound refer to $p = 5$ and $\Phi = \Phi_2$.

N^{du}	$\varepsilon_{N^{\text{du}}}^{\Psi,\text{rel}}$	$\Delta_{N^{\text{du}}}^{\Psi,\text{rel}}$	$\eta_{N^{\text{du}}}^{\Psi}$
5	6.01E-02	2.30E-01	3.83
10	2.76E-03	5.70E-03	2.07
15	2.26E-05	4.52E-05	2.00
20	7.74E-08	1.76E-07	2.28

Table 3: Reduced basis approximation of the dual state: relative truth error $\varepsilon_{N^{\text{du}}}^{\Psi,\text{rel}}$, relative error bound $\Delta_{N^{\text{du}}}^{\Psi,\text{rel}}$ and effectivity $\eta_{N^{\text{du}}}^{\Psi}$ as a function of N^{du} .

the problem considered. We can obtain a specific desired accuracy of the output bound for different combinations of N^{pr} and N^{du} . Due to the faster convergence of the dual problem, however, the effect of increasing N^{du} is much larger than the effect of increasing N^{pr} . To obtain a maximum output bound of approximately 10%, we require either $N^{\text{pr}} = 30$ and $N^{\text{du}} = 5$ or $N^{\text{pr}} = 4$ and $N^{\text{du}} = 10$. We can thus considerably decrease N^{pr} — here, a factor of ≈ 7 — while we only have to double N^{du} to keep the same accuracy of the output bound.

We also note that the convergence curves only reach an accuracy of approximately 2E-04. At this point the interpolation error bound, i.e., the last term in (62), dominates the primal-dual output error bound. Thus, increasing N^{pr} or N^{du} has, at this point, no effect on the convergence of the output bound anymore. This is in contrast to the results for affine problems, where only the first term in (62) is present and the convergence curves thus keep decreasing without reaching a plateau. We note that this plateau effect is important in choosing an efficient combination of N^{pr} vs. N^{du} vs. M . As a general guideline, M should be large enough such that the interpolation

error is small enough and the last term in (62) has the same order of magnitude as the first term. Subsequently, N^{pr} and N^{du} can be chosen so as to minimize the computational cost involved. The actual values of N^{pr} , N^{du} , and M required to satisfy these goals, however, are strongly problem dependent.

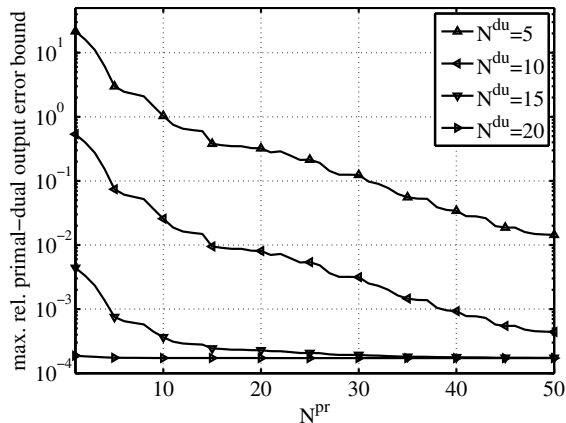


Figure 4: Numerical results for the reduced basis method: maximum relative primal-dual output error bound $\Delta_{M,N,\mathcal{P}}^{s,\text{max,rel}}$ as a function of N^{pr} for $N^{\text{du}} = 5, 10, 15, 20$, $M = 36$, $p = 5$ and $\Phi = \Phi_2$.

Finally, we present in Table 4 for a specific combination of N^{pr} , N^{du} , and M the maximum relative truth output errors $\varepsilon_{M,N}^{s,\text{max,rel}}$, the maximum relative output bound $\Delta_{M,N,\mathcal{P}}^{s,\text{max,rel}}$, and the average effectivity $\eta_{M,N,\mathcal{P}}^{s,\text{ave}}$; here, $\varepsilon_{M,N}^{s,\text{max,rel}}$ is the maximum over Ξ_{test} of $\varepsilon_{M,N}^{s,K}/|s^K|$, $\Delta_{M,N,\mathcal{P}}^{s,\text{max,rel}}$ is the maximum over Ξ_{test} of $\Delta_{M,N,\mathcal{P}}^{s,K}/|s^K(\mu)|$, and $\eta_{M,N,\mathcal{P}}^{s,\text{ave}}$ is the average over Ξ_{test} of $\Delta_{M,N,\mathcal{P}}^s(\mu)/\varepsilon_{M,N}^s(\mu)$. We also present the online computational times to calculate $s_{M,N}^k(\mu)$ and $\Delta_{N,M,\mathcal{P}}^{s,k}$ for $1 \leq k \leq K$. The values are normalized with respect to the computational time for direct calculation of the truth approximation output $s^k(\mu)$, $1 \leq k \leq K$. We present the corresponding results for the primal-only approach in Table 5.

We observe that the output approximation and output bound for the primal-dual formulation converge very fast. Furthermore, the primal-dual formulation is clearly superior to the primal-only formulation for the problem considered here. The reason, of course, is the parameter independence and thus fast convergence of the dual problem. To achieve a desired accuracy in the output bound of approximately 1%, we require $N^{\text{pr}} = 20$, $N^{\text{du}} = 10$, and $M = 20$ for the primal-dual formulation. Using the primal-only formulation the output bound is still larger than 10% even if we set N^{pr} and M to their maximum values $N_{\text{max}}^{\text{pr}} = M_{\text{max}} = 50$. The output effectivities are $\mathcal{O}(100)$ and thus

worse than the effectivities of the energy norm bounds since our bound cannot take into account any correlation between the primal and dual error. Despite the quite large effectivities, however, the computational savings are considerable: the computational time to evaluate the reduced basis output approximation *and* output bound is a factor of $\mathcal{O}(10^4)$ faster than direct calculation of the truth approximation output.

N^{pr}	N^{du}	M	$\varepsilon_{M,N}^{s,\text{max,rel}}$	$\Delta_{M,N,\mathcal{P}}^{s,\text{max,rel}}$	$\eta_{M,N,\mathcal{P}}^{s,\text{ave}}$	comp. time $\forall k$
10	5	10	6.59E-03	1.28E+00	599.62	6.09E-05
20	10	20	1.04E-04	9.50E-03	346.56	7.98E-05
30	15	30	3.74E-05	6.21E-04	813.41	1.05E-04

Table 4: Primal-dual reduced basis output approximation: maximum relative truth output error $\varepsilon_{M,N}^{s,\text{max,rel}}$, maximum relative output error bound $\Delta_{M,N,\mathcal{P}}^{s,\text{max,rel}}$, average effectivity $\eta_{M,N,\mathcal{P}}^{s,\text{ave}}$ and computation times for $p = 5$ and $\Phi = \Phi_2$ as a function of N^{pr} , N^{du} and M . The computation time is normalized with respect to the computation time of calculating the truth output.

N^{pr}	M	$\tilde{\varepsilon}_{M,N^{\text{pr}}}^{s,\text{max,rel}}$	$\tilde{\Delta}_{M,N^{\text{pr}},\mathcal{P}}^{s,\text{max,rel}}$	$\tilde{\eta}_{M,N^{\text{pr}},\mathcal{P}}^{s,\text{ave}}$	comp. time $\forall k$
5	10	2.41E-01	1.14E+01	257.26	2.34E-05
10	20	4.16E-02	2.87E+00	1585.89	3.01E-05
25	30	5.82E-03	6.84E-01	591.01	5.43E-05
40	36	1.11E-03	1.45E-01	562.08	8.39E-04

Table 5: Primal-only reduced basis output approximation: maximum relative truth output error $\tilde{\varepsilon}_{M,N^{\text{pr}}}^{s,\text{max,rel}}$, maximum relative output error bound $\tilde{\Delta}_{M,N^{\text{pr}},\mathcal{P}}^{s,\text{max,rel}}$, average effectivity $\tilde{\eta}_{M,N^{\text{pr}},\mathcal{P}}^{s,\text{ave}}$ and computation time for $p = 5$ and $\Phi = \Phi_2$ as a function of M and N^{pr} . The computation time is normalized with respect to the computation time of calculating the truth output.

7. Conclusions

We have presented rigorous *a posteriori* error bounds for reduced basis approximations of problems with non-affine source terms. To this end, we employed the recently proposed rigorous *a posteriori* error bounds for the empirical interpolation method and we developed adjoint procedures to ensure rapid convergence of the reduced basis output approximation and associated error bound.

The error bounds take both error contributions — the error introduced by the reduced basis approximation *and* the error induced by the function interpolation — explicitly into account.

We presented numerical results for a welding process that showed the very fast convergence of the reduced basis approximation and associated error bounds. The computational savings in the online stage are considerable; we observed a speed-up of $\mathcal{O}(10^4)$ in the calculation of the output estimate and bound compared to direct calculation of the truth output.

The primal-dual formulation proved to be clearly superior to the primal-only formulation for our model problem. We note that a small interpolation error and thus large enough dimension of the EIM approximation space is essential in recovering the square effect in the output approximation and bound. The welding problem has proven an ideal application for the use of adjoint techniques — the parametric dependence enters only in the right hand side of the primal problem and thus does not show up in the dual problem. However, adjoint techniques are advantageous also for problems with a more general parameter dependence [14, 23, 34, 22] and our development is thus not restricted to the particular problem considered here.

A topic of future research is the application of the methods developed here in the solution of the inverse problem using real experimental data.

Appendix A. Proof of Proposition 2

For simplicity we shall omit the parameter-dependence of the state variables in our notation, i.e. we write y^k instead of $y^k(\mu)$ etc.

First we note that the dual of the output at time t^L , $L = 1, \dots, K$, satisfies

$$-m(v, \psi_L^{k'+1} - \psi_L^{k'}) + \Delta t a(v, \psi_L^{k'+(1-\theta)}; \mu) = 0 \quad (\text{A.1})$$

for all $v \in X$ and $k' = 1, \dots, L$, with final condition

$$m(v, \psi_L^{L+1}) = l(v) \quad (\text{A.2})$$

for all $v \in X$. We now choose $v = e_{M, N^{\text{pr}}}^{y, k'-1+\theta}$ in (A.1) and sum from $k' = 1$ to L to obtain

$$-\sum_{k'=1}^L m(e_{M, N^{\text{pr}}}^{y, k'-1+\theta}, \psi_L^{k'+1} - \psi_L^{k'}) + \Delta t \sum_{k'=1}^L a(e_{M, N^{\text{pr}}}^{y, k'-1+\theta}, \psi_L^{k'+(1-\theta)}; \mu) = 0, \quad (\text{A.3})$$

which can be rewritten in the form

$$\sum_{k'=1}^L m(e_{M,N^{\text{Pr}}}^{y,k'} - e_{M,N^{\text{Pr}}}^{y,k'-1}, \psi_L^{k'+(1-\theta)}) + \Delta t \sum_{k'=1}^L a(e_{M,N^{\text{Pr}}}^{y,k'-1+\theta}, \psi_L^{k'+(1-\theta)}; \mu) = m(e_{M,N^{\text{Pr}}}^{y,L}, \psi_L^{L+1}), \quad (\text{A.4})$$

where we used the fact that $e_{M,N^{\text{Pr}}}^{y,0} \equiv 0$. We now note from the final condition of the dual problem (A.2) that $m(e_{M,N^{\text{Pr}}}^{y,L}, \psi_L^{L+1}) = l(e_{M,N^{\text{Pr}}}^{y,L})$ to obtain

$$l(e_{N^{\text{Pr}}}^{y,L}) = \sum_{k'=1}^L m(e_{M,N^{\text{Pr}}}^{y,k'} - e_{M,N^{\text{Pr}}}^{y,k'-1}, \psi_L^{k'+(1-\theta)}) + \Delta t \sum_{k'=1}^L a(e_{M,N^{\text{Pr}}}^{y,k'-1+\theta}, \psi_L^{k'+(1-\theta)}; \mu). \quad (\text{A.5})$$

We next derive from (19) and (34) that the primal error satisfies

$$\begin{aligned} m(e_{M,N^{\text{Pr}}}^{y,k'} - e_{M,N^{\text{Pr}}}^{y,k'-1}, v) + \Delta t a(e_{M,N^{\text{Pr}}}^{y,k'-1+\theta}, v; \mu) \\ = \Delta t r_{N^{\text{Pr}}}^{y,k'}(v; \mu) + \Delta t f(v; g(\mu) - g_M(\mu))u^{k'-1+\theta} \end{aligned} \quad (\text{A.6})$$

for all $v \in X$ and $k' = 1, \dots, K$. Choosing $v = \psi_L^{k'+(1-\theta)}$ and summing from $k' = 1$ to L it follows that

$$\begin{aligned} \sum_{k'=1}^L m(e_{M,N^{\text{Pr}}}^{y,k'} - e_{M,N^{\text{Pr}}}^{y,k'-1}, \psi_L^{k'+(1-\theta)}) + \Delta t \sum_{k'=1}^L a(e_{M,N^{\text{Pr}}}^{y,k'-1+\theta}, \psi_L^{k'+(1-\theta)}; \mu) \\ = \Delta t \sum_{k'=1}^L r_{N^{\text{Pr}}}^{y,k'}(\psi_L^{k'+(1-\theta)}; \mu) + \Delta t \sum_{k'=1}^L f(\psi_L^{k'+(1-\theta)}; g(\mu) - g_M(\mu))u^{k'-1+\theta}. \end{aligned} \quad (\text{A.7})$$

From (A.5) and (A.7) we have

$$\begin{aligned} l(e_{N^{\text{Pr}}}^{y,L}) = \Delta t \sum_{k'=1}^L r_{N^{\text{Pr}}}^{y,k'}(\Psi^{K-L+k'+(1-\theta)}; \mu) \\ + \Delta t \sum_{k'=1}^L f(\Psi^{K-L+k'+(1-\theta)}; g(\mu) - g_M(\mu))u^{k'-1+\theta}, \end{aligned} \quad (\text{A.8})$$

where we used the shifting property of the dual (24). From the definition of the truth output, $s^k(\mu)$, the reduced basis output approximation, $s_{M,N}^k(\mu)$, and (A.8) we now obtain

$$\begin{aligned} s^k(\mu) - s_{M,N}^k(\mu) = \Delta t \sum_{k'=1}^k r_{N^{\text{Pr}}}^{y,k'}(e_{N^{\text{du}}}^{\Psi, K-k+k'+(1-\theta)}(\mu); \mu) \\ + \Delta t \sum_{k'=1}^k f(\Psi^{K-k+k'+(1-\theta)}(\mu); g(\mu) - g_M(\mu))u^{k'-1+\theta}. \end{aligned} \quad (\text{A.9})$$

Using the definition of the dual norm the first term of the right hand side of (A.9) is bounded by

$$\left| \Delta t \sum_{k'=1}^k r_{N^{\text{Pr}}}^{y,k'}(e_{N^{\text{du}}}^{\Psi, K-k+k'+(1-\theta)}(\mu); \mu) \right| \leq \Delta t \sum_{k'=1}^k \left\| r_{N^{\text{Pr}}}^{y,k'}(\cdot; \mu) \right\|_{X^*} \left\| e_{N^{\text{du}}}^{\Psi, K-k+k'+(1-\theta)}(\mu) \right\|_X, \quad (\text{A.10})$$

and using the Cauchy-Schwarz inequality it follows that

$$\left| \Delta t \sum_{k'=1}^k r_{N^{\text{Pr}}}^{y,k'}(e_{N^{\text{du}}}^{\Psi, K-k+k'+(1-\theta)}(\mu); \mu) \right| \leq \left(\frac{\Delta t}{\alpha_a^{\text{LB}}(\mu)} \sum_{k'=1}^k \left\| r_{N^{\text{Pr}}}^{y,k'}(\cdot; \mu) \right\|_{X^*}^2 \right)^{\frac{1}{2}} \times \left(\Delta t \alpha_a^{\text{LB}}(\mu) \sum_{k'=1}^k \left\| e_{N^{\text{du}}}^{\Psi, K-k+k'+(1-\theta)}(\mu) \right\|_X^2 \right)^{\frac{1}{2}}. \quad (\text{A.11})$$

By definition, the first term of the right hand side of (A.11) is equal to the error bound $\Delta_{N^{\text{Pr}}}^{yM,k}(\mu)$ of the affine primal problem (22), and the second term satisfies

$$\Delta t \alpha_a^{\text{LB}}(\mu) \sum_{k'=1}^k \left\| e_{N^{\text{du}}}^{\Psi, K-k+k'+(1-\theta)}(\mu) \right\|_X^2 \leq \left(\Delta_{N^{\text{du}}}^{\Psi, K-k+1}(\mu) \right)^2. \quad (\text{A.12})$$

We now turn to the second term of the right hand side of (A.9), which we can bound by

$$\begin{aligned} & \Delta t \sum_{k'=1}^k f(\Psi^{K-k+k'+(1-\theta)}(\mu); g(\mu) - g_M(\mu)) u^{k'-1+\theta} \\ & \leq \Delta t \sum_{k'=1}^k \left\| e_{N^{\text{du}}}^{\Psi, K-k+k'+(1-\theta)}(\mu) \right\|_X \sup_{v \in X} \frac{f(v; g(\mu) - g_M(\mu))}{\|v\|_X} \left| u^{k'-1+\theta} \right| \\ & \quad + \Delta t \sum_{k'=1}^k f(\Psi_{N^{\text{du}}}^{K-k+k'+(1-\theta)}(\mu); g(\mu) - g_M(\mu)) u^{k'-1+\theta}. \end{aligned} \quad (\text{A.13})$$

With the help of the rigorous EIM-bound $\delta_{M,p,\Phi}^g$ this can be simplified to

$$\begin{aligned} & \Delta t \sum_{k'=1}^k f(\Psi^{K-k+k'+(1-\theta)}(\mu); g(\mu) - g_M(\mu)) u^{k'-1+\theta} \\ & \leq \Delta t \delta_{M,p,\Phi}^g \|f(\cdot; 1)\|_{X^*} \sum_{k'=1}^k \left\| e_{N^{\text{du}}}^{\Psi, K-k+k'+(1-\theta)}(\mu) \right\|_X \left| u^{k'-1+\theta} \right| \\ & \quad + \Delta t \delta_{M,p,\Phi}^g \sum_{k'=1}^k \left| f(\Psi_{N^{\text{du}}}^{K-k+k'+(1-\theta)}(\mu); 1) u^{k'-1+\theta} \right|. \end{aligned} \quad (\text{A.14})$$

Finally, using the Cauchy-Schwarz inequality, the coercivity of a and the definition of the dual spatio-temporal energy norm and the dual error bound, we have

$$\Delta t \sum_{k'=1}^k \left\| e_{N^{\text{du}}}^{\Psi, K-k+k'+(1-\theta)}(\mu) \right\|_X \left| u^{k'-1+\theta} \right| \leq \Delta_{N^{\text{du}}}^{\Psi, K-k+1}(\mu) \left(\frac{\Delta t}{\alpha_a^{\text{LB}}(\mu)} \sum_{k'=1}^k \left(u^{k'-1+\theta} \right)^2 \right)^{\frac{1}{2}}. \quad (\text{A.15})$$

The result directly follows from (A.9)-(A.15). \square

Acknowledgements

This work was supported by the Excellence Initiative of the German federal and state governments and the German Federation of Industrial Research Associations funded by the German Federal Ministry of Economics and Technology.

References

- [1] T. W. Eagar, N. S. Tsai, Temperature fields produced by traveling distributed heat sources, *Welding Journal* 62 (1983) S346–S355.
- [2] J. Goldak, M. Bibby, J. Moore, R. House, B. Patel, Computer modeling of heat flows in welds, *Metall. Mater. Trans. B* 17B (1985) 587–600.
- [3] J.-B. Song, D. E. Hardt, Dynamic modeling and adaptive control of the gas metal arc welding process, *Journal of Dynamics Systems, Measurement, and Control* 116 (1994) 405–413.
- [4] S. Wang, J. Goldak, J. Zhou, S. Tchernov, D. Downey, Simulation on the thermal cycle of a welding process space-time convection-diffusion finite element analysis, *International Journal of Thermal Sciences* 48 (2009) 936–947.
- [5] K. Kazemi, J. Goldak, Numerical simulation of laser full penetration welding, *Computational Materials Science* 44 (2009) 841–849.
- [6] J. Goldak, A. Chakravarti, M. Bibby, A new finite element model for welding heat sources, *Metall. Mater. Trans. B* 15B (1984) 299–305.
- [7] V. A. Karkhin, P. N. Homich, V. G. Michailov, Models for volume heat sources and functional-analytical technique for calculating the temperature fields in butt welding, in: *Mathematical Modelling of Weld Phenomena* 8, Verlag der Technischen Universität Graz, 2007, pp. 819–834.
- [8] V. Akçelik, G. Biros, A. Drăgănescu, O. Ghattas, J. Hill, B. van Bloemen Waanders, Dynamic data driven inversion for terascale simulations: Real-time identification of airborne contaminants, in: *Proceedings of the 2005 ACM/IEEE Conference on Supercomputing*.
- [9] O. Bashir, K. Willcox, O. Ghattas, B. van Bloemen Waanders, J. Hill, Hessian-based model reduction for large-scale systems with initial-condition inputs, *Int. J. Numer. Meth. Engng.* 73 (2008) 844–868.

- [10] L. Dede, A. Quarteroni, Optimal control and numerical adaptivity for advection-diffusion equations, *ESAIM: M2AN* 39 (2005) 1019–1040.
- [11] V. A. Karkhin, V. V. Plochikhine, H. W. Bergmann, Solution of inverse heat conduction problem for determining heat input, weld shape, and grain structure during laser welding, *Science and Technology of Welding and Joining* 7 (2002) 224–231.
- [12] J.-B. Song, D. E. Hardt, Closed-loop control of weld pool depth using a thermally based depth estimator, *Welding Journal* 72 (1993) S471–S478.
- [13] J.-B. Song, D. E. Hardt, Estimation of weld bead depth for in-process control, in: *Automation of Manufacturing Processes*, volume DSC-22 of *ASME Winter Annual Meeting*, pp. 39–45.
- [14] G. Rozza, D. Huynh, A. Patera, Reduced basis approximation and a posteriori error estimation of affinely parametrized elliptic coercive partial differential equations, *Archives of Computational Methods in Engineering* 15 (2008) 229–275.
- [15] M. Barrault, Y. Maday, N. C. Nguyen, A. T. Patera, An empirical interpolation method: Application to efficient reduced-basis discretization of partial differential equations, *CR Acad Sci Paris Series I* 339 (2004) 667–672.
- [16] M. A. Grepl, Y. Maday, N. C. Nguyen, A. T. Patera, Efficient reduced-basis treatment of nonaffine and nonlinear partial differential equations, *ESAIM: M2AN* 41 (2007) 575–605.
- [17] T. M. Lassila, G. Rozza, Parametric free-form shape design with pde models and reduced basis method, *Computer Methods in Applied Mechanics and Engineering* 199 (2010) 1583–1592.
- [18] C. Canuto, T. Tonn, K. Urban, A-posteriori error analysis of the reduced basis method for non-affine parameterized nonlinear pde’s, *SIAM J. Numer. Anal.* 47 (2009) 2001–2022.
- [19] N. C. Nguyen, A posteriori error estimation and basis adaptivity for reduced-basis approximation of nonaffine-parametrized linear elliptic partial differential equations, *Journal of Computational Physics* 227 (2007) 983–1006.
- [20] M. A. Grepl, A posteriori error bounds for reduced basis approximations of nonaffine and nonlinear parabolic partial differential equations, 2010. Submitted to *Math. Mod. Meth. Appl. Sc.*
- [21] J. L. Eftang, M. A. Grepl, A. T. Patera, A posteriori error bounds for the empirical interpolation method, *CR Acad Sci Paris Series I* 348 (2010) 575–579.
- [22] D. V. Rovas, L. Machiels, Y. Maday, Reduced-basis output bound methods for parabolic problems, *IMA Journal of Numerical Analysis* 26 (2006) 423–445.
- [23] M. Grepl, A. Patera, A posteriori error bounds for reduced-basis approximations of parametrized parabolic partial differential equations, *ESAIM: M2AN* 39 (2005) 157–181.
- [24] Y. Maday, N. C. Nguyen, A. T. Patera, G. S. H. Pau, A general multipurpose interpolation procedure: The magic points, *Comm. Pure Appl. Anal.* 8 (2009) 383–404.
- [25] A. Quarteroni, R. Sacco, F. Saleri, *Numerical Mathematics*, volume 37 of *Texts in Applied Mathematics*, Springer, New York, 1991.
- [26] J. Eftang, M. Grepl, A. Patera, E. Rønquist, Approximation of parametric derivatives by the empirical interpolation method, In preparation (2011).
- [27] A. Quarteroni, A. Valli, *Numerical Approximation of Partial Differential Equations*, Springer, 2nd edition, 1997.
- [28] R. Becker, R. Rannacher, Weighted a posteriori error control in finite element methods, in: *ENUMATH 95*

Proc, World Sci. Publ. Singapore, 1997.

- [29] D. B. P. Huynh, G. Rozza, S. Sen, A. Patera, A successive constraint linear optimization method for lower bounds of parametric coercivity and inf-sup stability constants, *CR Acad Sci Paris Series I* 345 (2007) 473–478.
- [30] C. Prud'homme, D. Rovas, K. Veroy, Y. Maday, A. T. Patera, G. Turinici, Reliable real-time solution of parametrized partial differential equations: Reduced-basis output bound methods, *Journal of Fluids Engineering* (2002) 70–80.
- [31] K. Veroy, D. Rovas, A. T. Patera, A posteriori error estimation for reduced-basis approximation of parametrized elliptic coercive partial differential equations: “Convex inverse” bound conditioners, *Control, Optimisation and Calculus of Variations* 8 (2002) 1007–1028. Special Volume: A tribute to J.-L. Lions.
- [32] B. Haasdonk, M. Ohlberger, Reduced basis method for finite volume approximations of parametrized linear evolution equations, *M2AN Math. Model. Numer. Anal.* 42 (2008) 277–302.
- [33] L. Sirovich, Turbulence and the dynamics of coherent structures, part 1: Coherent structures, *Quarterly of Applied Mathematics* 45 (1987) 561–571.
- [34] K. Veroy, A. T. Patera, Certified real-time solution of the parametrized steady incompressible navier-stokes equations: rigorous reduced-basis a posteriori error bounds, *Int. J. Num. Meth. Fluids* 47 (2005) 773–788.